Cell Reports

Article

Quantitative differences between cyclin-dependent kinases underlie the unique functions of CDK1 in human cells

Graphical abstract

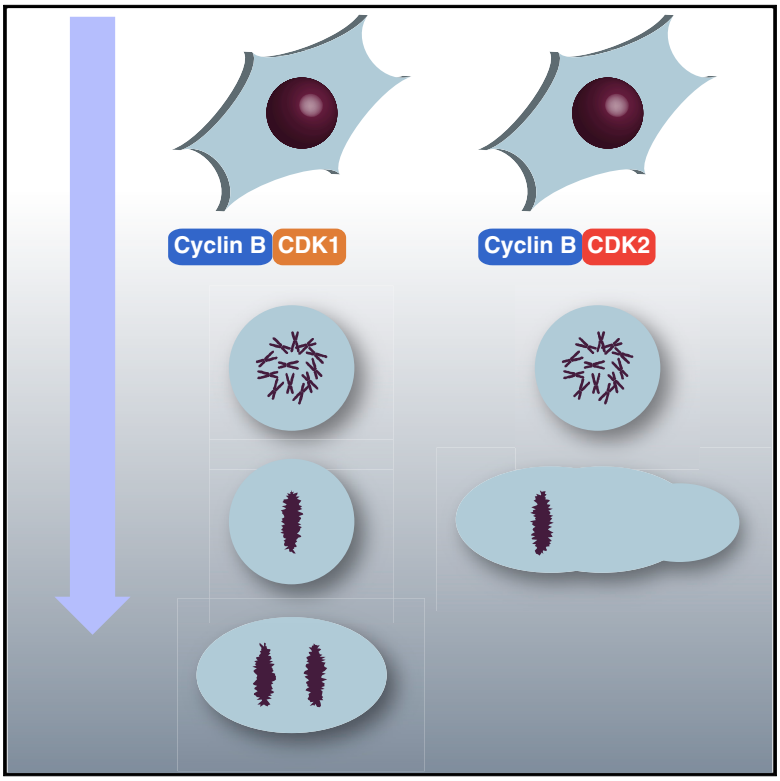

Highlights

- CDK1 deficiency blocks mitotic entry in normal RPE1 cells, not in cancer cell lines
- Cyclin B-CDK2 assumes the role of an M phase-promoting factor in the absence of CDK1
- Low abundance of CDK2 accounts for defective mitotic progression in CDK1-deficient cells
- Ectopic expression of CDK2 can rescue CDK1's functions in mitosis in human cell lines

Authors

Ho Wai Lau, Hoi Tang Ma, Tsz Kwan Yeung, Man Yee Tam, Danyi Zheng, Siu Ki Chu, Randy Yat Choi Poon

Correspondence

rycpoon@ust.hk

In brief

The reason for the presence of a single CDK in yeast but multiple CDKs in higher eukaryotes remains unknown. Lau et al. show that the classic mitotic CDK1's functions can be replaced by overexpressed CDK2 in human cell lines.

Lau et al., 2021, Cell Reports *37*, 109808
October 12, 2021
https://doi.org/10.1016/j.celrep.2021.109808

CellPress

Cell Reports

CellPress
OPEN ACCESS

Article

Quantitative differences between cyclin-dependent kinases underlie the unique functions of CDK1 in human cells

Ho Wai Lau,[1,3] Hoi Tang Ma,[1,3] Tsz Kwan Yeung,[1] Man Yee Tam,[1] Danyi Zheng,[1] Siu Ki Chu,[1] and Randy Yat Choi Poon[1,2,4,*]

[1]Division of Life Science, Hong Kong University of Science and Technology, Clear Water Bay, Hong Kong
[2]Center for Cancer Research and State Key Laboratory of Molecular Neuroscience, Hong Kong University of Science and Technology, Clear Water Bay, Hong Kong
[3]These authors contributed equally
[4]Lead contact
*Correspondence: rycpoon@ust.hk
https://doi.org/10.1016/j.celrep.2021.109808

SUMMARY

One of the most intriguing features of cell-cycle control is that, although there are multiple cyclin-dependent kinases (CDKs) in higher eukaryotes, a single CDK is responsible for both G_1-S and G_2-M in yeasts. By leveraging a rapid conditional silencing system in human cell lines, we confirm that CDK1 assumes the role of G_1-S CDK in the absence of CDK2. Unexpectedly, CDK1 deficiency does not prevent mitotic entry. Nonetheless, inadequate phosphorylation of mitotic substrates by noncanonical cyclin B-CDK2 complexes does not allow progression beyond metaphase and underscores deleterious late mitotic events, including the uncoupling of anaphase A and B and cytokinesis. Elevation of CDK2 to a level similar to CDK1 overcomes the mitotic defects caused by CDK1 deficiency, indicating that the relatively low concentration of CDK2 accounts for the defective anaphase. Collectively, these results reveal that the difference between G_2-M and G_1-S CDKs in human cells is essentially quantitative.

INTRODUCTION

The cell cycle is choreographed by an evolutionarily conserved engine composed of a family of protein kinases called cyclin-dependent kinases (CDKs) (Poon, 2016). The activities of CDKs are stringently regulated by protein-protein interactions and phosphorylation. In particular, binding to a cyclin subunit is necessary for full activation of CDKs. Conversely, ubiquitin-mediated destruction of cyclins provides a rapid way to inactivate CDKs and is critical for many cell-cycle transitions.

The current paradigm states that in human cells, CDK1 forms complexes with the mitotic cyclins (cyclin A and B) and drives G_2 cells into mitosis (Fung and Poon, 2005). Another member of the CDK family, CDK2, associates mainly with cyclin E and cyclin A, and the complexes formed are critical for G_1-S transition and in S phase, respectively (Woo and Poon, 2003). CDK4 and CDK6 are partners of cyclin D, functioning in G_1 before cyclin E-CDK2. The prime target of cyclin D-CDK4/6 is the retinoblastoma gene product pRb. Hyperphosphorylation of pRb by CDK4/6 (and by CDK2) releases pRb from E2F, empowering E2F to activate transcription of genes critical for S phase (Malumbres, 2014).

A cornerstone in cell-cycle control is the highly conserved nature of CDKs in eukaryotic cells. Regulation of CDKs is conserved down to the molecular details between lower and higher eukaryotes. However, one of the most interesting aspects is that although there are multiple CDKs in higher eukaryotes, a single CDK is responsible for both G_1-S and G_2-M in yeasts (by contrast, there are multiple cyclins in both yeast and human). In fact, one of the defining studies in the field of cell-cycle control is the discovery that human CDK1 can complement the functions of budding yeast Cdc2 (the only cell-cycle CDK present in *S. pombe*) (Lee and Nurse, 1987).

Studies using CDK-deficient mice have been pivotal in revealing the possible unique and redundant roles of various CDKs in mammalian cells. Although knockout (KO) of CDK1 in mice is embryonic lethal (Santamaría et al., 2007), CDK2-KO mice survived and developed normally (except for being sterile) (Berthet et al., 2003; Ortega et al., 2003). In CDK2-KO cells, CDK1 can replace CDK2 to form an active complex with cyclin E to orchestrate G_1-S (Aleem et al., 2005; Satyanarayana et al., 2008b). CDK4 and CDK6 are also non-essential for cell-cycle progression, because CDK4,6 double-KO mice die only during late stages of embryonic development as a result of severe anemia (Malumbres et al., 2004). In fact, CDK1 appears to be able to perform the functions of other CDKs in mice lacking all interphase CDKs (Santamaría et al., 2007). These mouse studies challenged the indispensable roles of different CDKs during the cell cycle and revealed possible compensation between members of the CDK family.

Given that CDK1 is the only essential cell-cycle CDK in mice, why metazoans contain multiple cell-cycle CDKs is a long-standing puzzle. With the high degree of similarity between

CDK1 and CDK2, it is intriguing that CDK1 can compensate for the loss of CDK2, but not vice versa. At least in budding yeast, mammalian CDK2 can compensate for the loss of yeast CDK, including during mitosis (Ninomiya-Tsuji et al., 1991; Meyerson et al., 1992; Elledge et al., 1992). Because ^{KO}CDK1 mice die during early embryonic development, a major unanswered question is the precise stage(s) of the cell cycle at which CDK1-deficient cells are arrested. Another limitation of CDK KO mouse experiments is the possibility of altered gene expression that promotes long-term compensation.

If there are gaps in our knowledge regarding the roles of CDKs in mouse cells, even less is unambiguously defined about the unique and redundant roles of various CDKs in human cells. Moreover, because CDK pathways are entirely rewired in human cancer (including alteration of expression of CDKs, cyclins, CDK regulators, and downstream CDK targets by genetic and epigenetic mechanisms), the precise relationship between different CDKs in cancer cells remains ambiguous.

Although there is considerable literature on loss-of-function studies of CDKs in human cell lines, they are limited by the technology available at the time, which generally involved chemical inhibitors or RNAi-mediated knockdown. In addition to the issue of specificity, major drawbacks of RNAi-mediated studies of CDKs include the incompleteness and slow kinetics of knockdown. The issue of specificity of small chemical inhibitors of CDKs also prevents unequivocal conclusions to be drawn from their use. Moreover, because small chemical inhibitors and chemical genetics approaches abolish CDKs' kinase activity, their cellular effects are not necessarily equivalent to the loss of CDKs. It is likely that although inactive CDKs are locked in complexes with their cyclin partners, deletion of CDKs could facilitate redistribution of the cyclins to alternative CDKs. For example, chemical genetic approaches (in which CDK2 is replaced with an analog-sensitive allele) indicate that the activity of CDK2 is essential for both passage through Restriction (R) point and S phase entry (Merrick et al., 2011), suggesting that CDK1 can replace CDK2's function only when the amount of CDK2 protein is lowered to free its cyclin partners.

Although the conventional view is that the essential function of CDK1 in mitosis cannot be compensated by other CDKs, it is likely too simplistic a view for many cancer cells. We hypothesize that the presence of multiple CDKs and epigenetic rewiring may provide cancer cells the plasticity to use alternative CDKs to orchestrate the cell cycle. With the availability of newer and more precise tools, including CRISPR-Cas9 and degron-mediated conditional gene inactivation, CDKs can be rapidly removed from human cell lines either individually or in combination. Our experiments revealed unexpected effects of CDK1 deficiency, the role of CDK2 in mitosis, as well as intriguing differences between cancer and normal cell lines.

RESULTS

CDK1, but not CDK2, is essential in human cell lines

We recently developed a conditional deficiency system with a dual-transcription/degron switch for studying potential essential genes, such as CDKs (Yeung et al., 2021; Ng et al., 2019). CDKs fused with auxin-inducible degron (AID) were expressed at the same time as when the endogenous CDK genes were ablated using CRISPR-Cas9. ^{AID}CDKs could then be degraded rapidly in response to indole-3-acetic acid (IAA) in cells expressing the ubiquitin ligase SCF^{TIR1}. Because ^{AID}CDKs were placed under the control of a Tet-Off promoter, the transcription of ^{AID}CDKs could also be suppressed with doxycycline (Dox). By combining both Dox and IAA together (DI herein), ^{AID}CDKs can be depleted quicker and more tightly than the individual chemicals alone (Ng et al., 2019). ^{AID}CDKs were generally reduced to an undetectable level within 3 h after addition of DI (see later in Figure S3D).

We first generated HeLa cells expressing AID-tagged CDK1 or CDK2 in the corresponding KO background (^{AID}CDK1^{KO}CDK1 and ^{AID}CDK2^{KO}CDK2, respectively). Single colony-derived clones were isolated that were deficient in endogenous CDK and expressed ^{AID}CDK at a comparable level as the endogenous CDK in the parental cells (Figures 1A and S1A). Using a serially diluted standard curve for immunoblotting, we estimated that the expression of ^{AID}CDK1 after DI treatment was less than 1% of the endogenous CDK1 (Figure S1B).

Flow cytometry analysis indicated that the cell-cycle distribution of ^{AID}CDK2^{KO}CDK2 was not altered after DI treatment. By contrast, the same treatment resulted in cell-cycle delay with 4N DNA content (indicative of G_2/M/mitotic slippage) in ^{AID}CDK1^{KO}CDK1 cells (Figure 1B). Bromodeoxyuridine (BrdU) incorporation assay further revealed that the cell-cycle delay was not due to a delay in late S (Figure 1C). The same results were obtained when the experiments were repeated using ^{AID}CDK1^{KO}CDK1 generated from H1299, indicating that the effects were not restricted to HeLa (Figures S1C and S1D). Clonogenic survival assay further showed that long-term survival was attenuated in the absence of CDK1, but not CDK2 (although the colonies were smaller without CDK2) (Figure 1D).

Collectively, these data confirmed that removal of CDK1 resulted in erroneous G_2/M control. By contrast, the loss of CDK2 does not affect cell-cycle progression, suggesting that the normal functions of CDK2 can be compensated for by other CDKs.

CDK1 is not required for mitotic entry but is essential for proper coordination of anaphase and cytokinesis

We next tracked individual cells using live-cell imaging to demarcate the precise defects in ^{KO}CDK1. Unexpectedly, ^{AID}CDK1^{KO}CDK1 cells were able to enter mitosis after the addition of DI, indicating that the above flow cytometry results were not due to a blockage of G_2-M. To assess whether mitotic entry was delayed, we synchronously released ^{AID}CDK1^{KO}CDK1 cells from a mitotic block before addition of DI at different time points. Figure 2A shows that cells treated with DI as soon as they were released from mitosis were still able to enter the subsequent mitosis, albeit with a delay of ~2 h (quantified in Figure S2A).

Although CDK1-deficient cells could enter mitosis, they exhibited a highly erroneous form of mitosis. The duration from DNA condensation to anaphase A was 58% longer in CDK1-deficient cells than control (Figure 2B). By contrast, the absence of CDK2 affected neither the duration of interphase nor mitosis. A similar prolonged mitosis was observed in ^{KO}CDK1 H1299 (the interphase delay was more pronounced in H1299 than in HeLa) (Figure S2B).

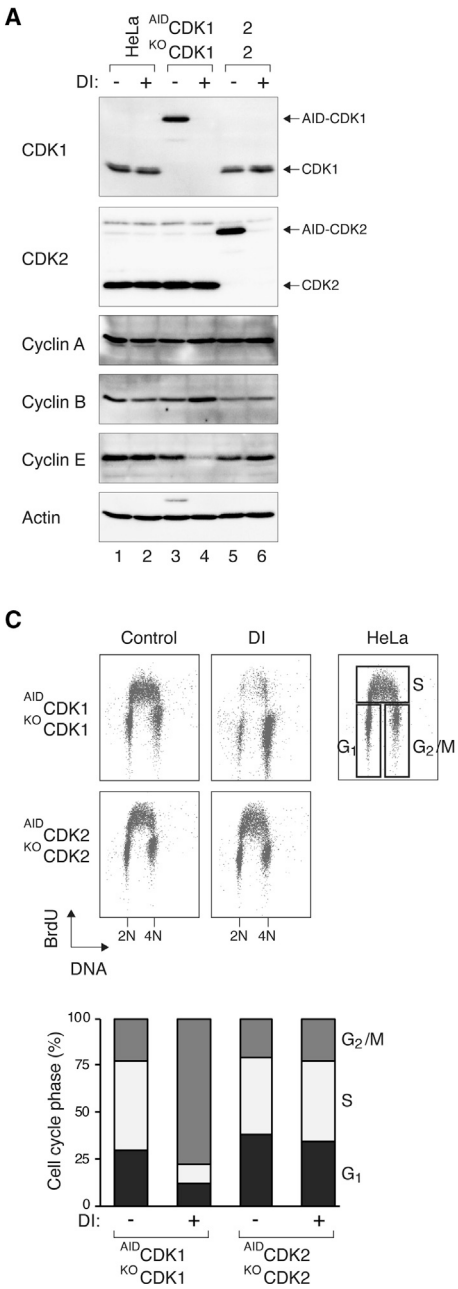

Figure 1. CDK1, but not CDK2, is essential for HeLa cell survival

(A) Conditional silencing of CDK1 or CDK2 by leveraging both transcriptional and degron-mediated control. HeLa, ^{AID}CDK1^{KO}CDK1, or ^{AID}CDK2^{KO}CDK2 cells were incubated in the absence or presence of DI (to turn on or off ^{AID}CDKs, respectively). After 24 h, lysates were prepared, and the indicated proteins were detected with immunoblotting. Actin analysis was included to assess protein loading and transfer (the extra band in lane 3 is a signal from the CDK1 blot). The relative size of the endogenous CDKs and ^{AID}CDKs is shown in Figure S1A.

(B) Defective cell-cycle progression after silencing of CDK1 (but not CDK2). Cells were treated as in (A) and harvested for flow cytometry analysis. The positions of 2N and 4N DNA contents are indicated.

(C) Enrichment of cells with 4N DNA after turning off of CDK1. Cells were grown in the presence or absence of DI for 23.5 h before being pulsed with BrdU for 30 min. BrdU incorporation and DNA contents were analyzed with bivariate flow cytometry. The positions of different cell-cycle populations are indicated for HeLa cells. The percentage of cells in different cell-cycle phase was quantified (bottom panel).

(D) Silencing of CDK1 abolishes cell survival. Clonogenic survival assays were performed in the presence or absence of DI. The number of colonies was quantified after ~2 weeks. Examples of plates after staining are shown. Mean ± SEM of three independent experiments.

During normal mitosis, anaphase A (sister chromatid separation) is followed immediately by anaphase B (elongation of the spindle, increased distance between the spindle poles, and transformation of the cell shape from a spherical to an oblong capsule). Intriguingly, the normal order of anaphase A and B was reversed in the absence of CDK1 (Figure 2C). Anaphase A was markedly delayed, while anaphase B was accelerated, resulting in anaphase B occurring before anaphase A (Figure 2D). As the cell elongated, the metaphase plate oscillated along the long axis of the cell with a frequency varying from 20 to 60 min (Figure 2E). Multiple cytokinesis-like events took place at locations where the metaphase plate passed, resulting in partial or complete formation of cell bodies (without DNA) (Figures 2D and 2F). The intercentrosome distance remained relatively constant, while the total cell length increased (Figure 2F), indicating that the entire spindle and metaphase plate oscillated along the axis. When sister chromatid separation eventually took place, it was frequently characterized by the presence of chromosomal bridges and lagging chromosomes (Figure 2F). Inhibition of the extensive cell death following the defective mitosis with a caspase inhibitor resulted in an accumulation of cells with 8N DNA content, indicating the cells could undergo DNA re-replication if apoptosis was inhibited (Figure S2C).

The delay of anaphase A in CDK1-deficient cells suggested that anaphase-promoting complex/cyclosome (APC/C) was not activated on time. An APC/C biosensor consisting of mRFP fused with the D-box of cyclin B1 was used to analyze the activity of APC/C. During normal mitosis, the APC/C biosensor was degraded after the onset of sister chromatid separation (Figure 2G). In CDK1-deficient cells, APC/C remained inactive during cell elongation and metaphase plate oscillation, suggesting that activation of APC/C may be impaired without CDK1.

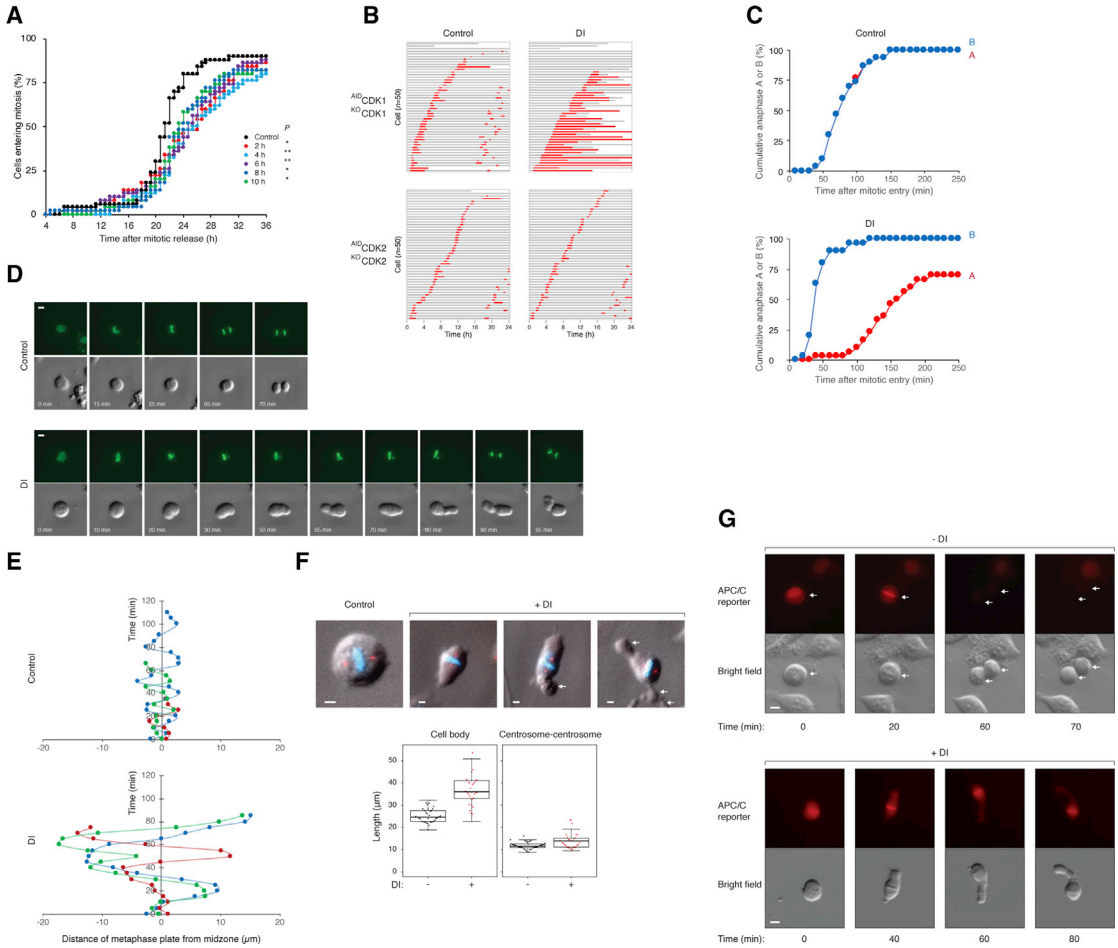

Figure 2. Loss of CDK1 uncouples normal anaphase

(A) Loss of CDK1 delays interphase progression but does not abolish mitotic entry. ^{AID}CDK1^{KO}CDK1 cells were synchronized at mitosis with NOC shake-off and released into the cell cycle. The cells were either untreated or incubated with DI at the indicated time points after release before being tracked using live-cell imaging (starting at 4 h after mitotic release). The percentage of cells entering mitosis over time was quantified (n = 50 for each sample). *p < 0.05, **p < 0.01 compared with control.

(B) CDK1 deficiency results in abnormally long mitosis and cell death. ^{AID}CDK1^{KO}CDK1 or ^{AID}CDK2^{KO}CDK2 cells were incubated in medium without or containing DI. The cells were subjected to live-cell imaging analysis for 24 h. Key: interphase, gray; mitosis, red; truncated bars, death.

(C) Uncoupling of the timing of anaphase A and anaphase B in CDK1-deficient cells. ^{AID}CDK1^{KO}CDK1 cells transfected with a plasmid expressing histone H2B-GFP were incubated in medium without or containing DI before being analyzed with live-cell imaging. The time of anaphase A and anaphase B relative to mitotic entry was quantified.

(D) Impaired mitosis in the absence of CDK1. ^{AID}CDK1^{KO}CDK1 cells transfected with a plasmid expressing histone H2B-GFP were incubated in medium without or containing DI before being analyzed with live-cell imaging. Examples of a control and a CDK1-depleted cell are shown. Signals from histone H2B-GFP (green) and bright field are shown (scale bars: 10 μm).

(E) Oscillation of metaphase plate in CDK1-deficient cells. ^{AID}CDK1^{KO}CDK1 cells were treated and analyzed with live-cell imaging as in (A). The distance of the metaphase plate from the midzone of the cell (the midpoint of the longest axis) at different time points after the formation of metaphase plate was measured. Examples of control and DI-treated cells (three each) are shown.

(F) Cell elongation without anaphase A in CDK1-deficient cells. ^{AID}CDK1^{KO}CDK1 cells were incubated in medium without or containing DI for 24 h before being fixed and analyzed with immunofluorescence microscopy (blue: DNA; red: pericentrin; overlay with bright field). Examples of cells with metaphase plate in a control and CDK1-deficient cells are shown (scale bars: 5 μm). Note that premature anaphase B and partial cytokinesis (arrows) occurred in CDK1-deficient cells. The length of the cell body (the longest axis) and centrosome-centrosome distance are quantified (n = 40).

(G) Impaired APC/C activation in the absence of CDK1. ^{AID}CDK1^{KO}CDK1 cells were transfected with an APC/C biosensor. The cells were incubated in medium without or containing DI and analyzed with live-cell imaging (scale bars: 5 μm).

Collectively, these unanticipated results indicate that CDK1 deficiency in human cell lines results in a transient interphase delay but does not prevent mitotic entry. The ensuing mitosis displays multiple defects, including a delay of anaphase A, as well as a loss of coordination between anaphase A, anaphase B, and cytokinesis.

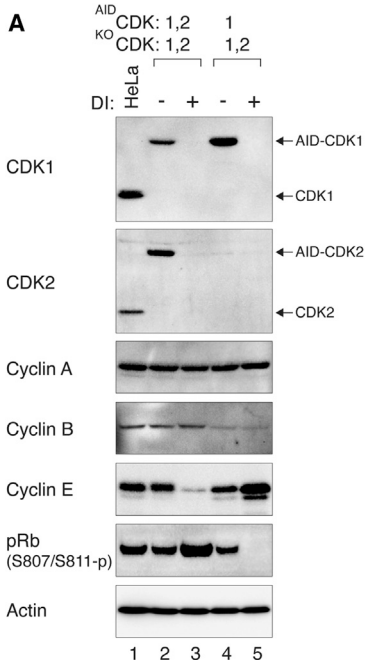

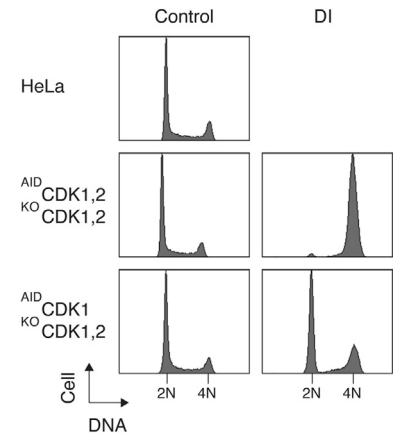

Figure 3. CDK2 assumes the role of a mitotic kinase in the absence of CDK1

(A) Concurrent silencing of CDK1 and CDK2. Cells expressing either ^{AID}CDK1 and ^{AID}CDK2 together (lanes 2–3) or ^{AID}CDK1 only (lanes 4–5) in ^{KO}CDK1,2 background were generated. The cells were incubated with or without DI. After 24 h, lysates were prepared, and the indicated proteins were detected with immunoblotting. Lysates from HeLa cells were loaded to indicate the relative expression of endogenous proteins.

(B) CDK1 and CDK2 control both G_1/S and G_2/M. HeLa, ^{AID}CDK1^{KO}CDK1,2, and ^{AID}CDK1,2^{KO}CDK1,2 were incubated with or without DI. After 24 h, the cells were harvested for flow cytometry analysis.

CDK2 becomes a mitotic kinase in the absence of CDK1

From the above results, we hypothesized that CDK2 can replace the functions of CDK1, at least up until metaphase. The next logical step to test this hypothesis was to further remove CDK2 in ^{AID}CDK1^{KO}CDK1 cells, with the expectation of abolishing mitosis altogether. The double CDK1,2 KO cells (^{AID}CDK1^{KO}CDK1,2) proliferated normally, consistent with the non-essential nature of CDK2 when CDK1 was present. Turning off ^{AID}CDK1 in these cells effectively produced a CDK1,2 double-deficient environment (Figure 3A). A shortcoming of this strategy, however, is that the cells underwent a G_1 arrest (Figure 3B), possibly because ^{AID}CDK1 replaced the normal G_1-S functions of CDK2. Consistently, turning off ^{AID}CDK1 triggered an accumulation of cyclin E and a loss of pRb phosphorylation (Figure 3A). In further agreement with this, turning off ^{AID}CDK1 in cells synchronously released from mitosis triggered a G_1 arrest (Figure S3A). Addition of the microtubule inhibitor nocodazole (NOC) only slightly enriched mitotic cells, indicating that the G_1 arrest was relatively tight (Figure S3B). A similar G_1 arrest in ^{KO}CDK1,2 was obtained using H1299 as a model (Figure S4A). Accordingly, turning off ^{AID}CDK1 in ^{AID}CDK1^{KO}CDK1,2 generated from H1299 abolished mitosis (Figure S4B) and triggered a cell-cycle arrest in G_1 (Figure S4C). This is also consistent with the requirement of CDK2 for S phase in CDK1-deficient mouse hepatocytes (Dewhurst et al., 2020).

Interestingly, the G_1 arrest in ^{KO}CDK1,2 could be circumvented when both ^{AID}CDK1 and ^{AID}CDK2 were expressed (Figure 3A). Accordingly, ^{AID}CDK1,2^{KO}CDK1,2 cells were arrested with 4N DNA after both ^{AID}CDK1 and ^{AID}CDK2 were turned off (Figure 3B). Although progression through G_1 and S was slower than control (Figure S3A), the cells were eventually arrested in G_2 as revealed by flow cytometry (Figure S3B) and live-cell imaging (Figure S3C), supporting the hypothesis that either CDK1 or CDK2 is sufficient to drive G_2 cells into mitosis.

The difference in cell-cycle arrest between ^{AID}CDK1^{KO}CDK1,2 and ^{AID}CDK1,2^{KO}CDK1,2 (G_1 and G_2, respectively) was unexpected because both cell lines effectively became ^{KO}CDK1,2 after addition of DI. Both ^{AID}CDK1 and ^{AID}CDK2 were under identical controls and were undetectable after 3 h of treatment (Figure S3D). It has been proposed that a lower threshold of CDK activity is involved in driving S phase compared with that for mitosis (Stern and Nurse, 1996; Coudreuse and Nurse, 2010; Swaffer et al., 2016). It is possible that the presence of both CDK1 and CDK2 in early G_1 was sufficient to provide residual CDK activity that allowed passage through G_1-S. Although the precise molecular mechanism underlying the G_1-S regulation in these cell lines remains to be elucidated, these data unequivocally demonstrated that mitotic entry was abolished in the absence of both CDK1 and CDK2.

Cyclin B-CDK2 assumes the role of an M-phase-promoting factor in the absence of CDK1

To address how mitotic entry could occur without CDK1, we next examined the formation of different cyclin-CDK complexes after ablation of CDKs. Silencing of either CDK1 or CDK2 did not affect the expression of cyclin A and cyclin B (Figure 4A). Consistent with their unusually long G_2 and mitosis, CDK1-deficient cells expressed slightly more cyclin B and markedly less cyclin E compared with CDK1-expressing cells.

The binding of cyclins to CDK1 was analyzed by co-immunoprecipitation. Figure 4B shows that degradation of ^{AID}CDK2 in ^{AID}CDK2^{KO}CDK2 cells enhanced the binding of CDK1 to cyclin E (and to a smaller extent to cyclin A). These results suggest that in the absence of CDK2, cyclin E forms a complex with CDK1 and is likely to account for the normal G_1-S control.

We next examined the effects of CDK1 ablation on CDK2-containing complexes. Immunoprecipitation of CDK2 showed that the amount of cyclin B-CDK2 complexes increased markedly after ^{AID}CDK1 was destroyed in ^{AID}CDK1^{KO}CDK1 cells (Figure 4C). This was confirmed by the converse experiment of immunoprecipitating cyclin B (Figure 4D). A marginal increase in cyclin

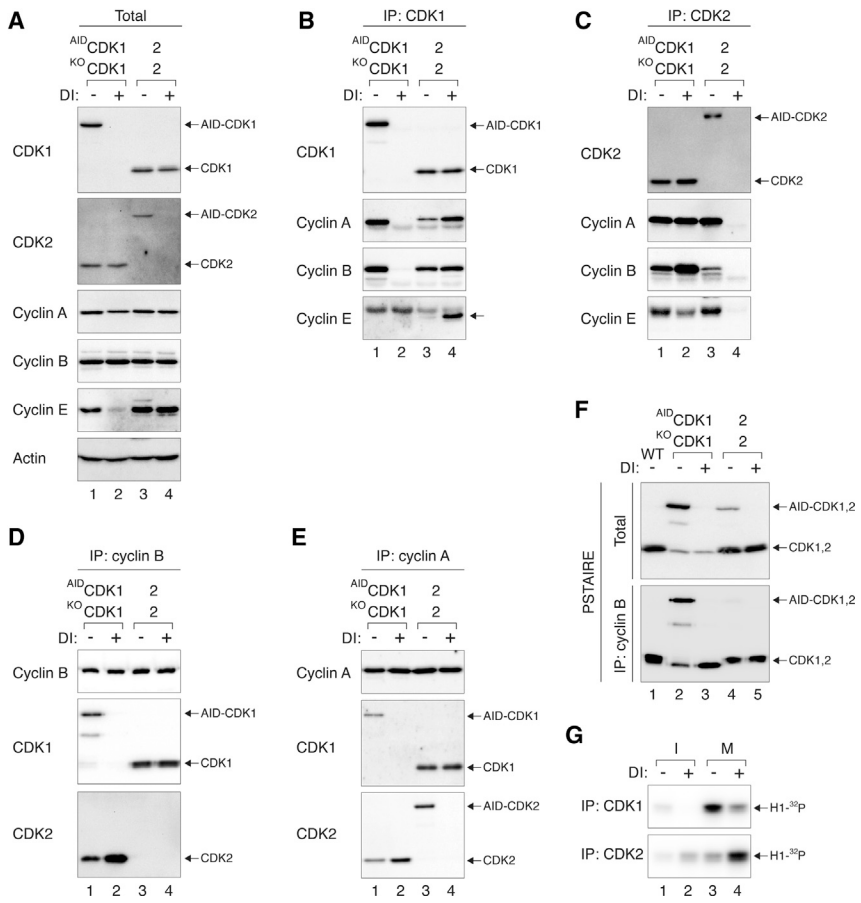

Figure 4. Binding of CDK2 to mitotic cyclins facilitates mitotic entry without CDK1

(A) The effects of depletion of CDK1 on the cell cycle are reflected by the expression of cyclins. ^{AID}CDK1^{KO}CDK1 or ^{AID}CDK2^{KO}CDK2 cells were incubated with or without DI for 24 h. The expression of the indicated proteins was analyzed with immunoblotting.

(B) Formation of cyclin E-CDK1 upon the loss of CDK2. Samples deficient in CDK1 or CDK2 were generated as described in (A). The lysates were subjected to immunoprecipitation using antibodies against CDK1. CDK1 (both ^{AID}CDK1 and endogenous CDK1) and different cyclins in the immunoprecipitates were detected with immunoblotting.

(C) Increase of cyclin B-CDK2 upon the loss of CDK1. The experiment was performed as in (B) except that antibodies against CDK2 were used for immunoprecipitation.

(D) Increase of cyclin B-CDK2 upon the loss of CDK1. The experiment was performed as in (B) except that antibodies against cyclin B were used for immunoprecipitation.

(E) Increase of cyclin A-CDK2 upon the loss of CDK1. The experiment was performed as in (B) except that antibodies against cyclin A were used for immunoprecipitation.

(F) ^{KO}CDK1 cells accumulate a similar level of cyclin B-CDK2 as cyclin B-CDK1 in normal cells. HeLa (wild-type [WT]), ^{AID}CDK1^{KO}CDK1, or ^{AID}CDK2^{KO}CDK2 cells were incubated with or without DI for 24 h. Lysates were prepared and subjected to immunoprecipitation using antibodies against cyclin B. Both the total lysates and immunoprecipitates were analyzed with immunoblotting for PSTAIRE (an epitope present in both CDK1 and CDK2).

(G) Increase of the kinase activity of CDK2 upon the loss of CDK1. ^{AID}CDK1^{KO}CDK1 cells incubated with or without DI were enriched in mitosis (M; NOC-blocked) or interphase (I; asynchronous cells washed with PBS before harvest). The lysates were subjected to immunoprecipitation using antibodies against CDK1 or CDK2. The kinase activities were measured using histone H1 as a substrate.

A-CDK2 complexes could also be detected after CDK1 degradation (Figures 4C and 4E). Similar results were obtained using H1299, indicating that the observations were not limited to one cell type (Figures S5A and S5B). Unlike after the removal of ^{AID}CDK1 with DI, inhibition of the kinase activity of ^{AID}CDK1 using a small-molecule inhibitor (RO3306) did not result in an increase in cyclin B-CDK2 complexes (Figure S5D). These results highlighted the conceptual differences between KO and inhibition of CDK1 as stated in the beginning of this study.

To interrogate the relative abundance of cyclin B-CDK2 in relationship with cyclin B-CDK1, we make use of a PSTAIRE monoclonal antibody, which recognizes an epitope present in both CDK1 and CDK2. Because CDK1 and CDK2 are very similar in size, they could not be readily resolved on SDS-PAGE. We reasoned that because endogenous CDK1 was absent in ^{AID}CDK1^{KO}CDK1 cells, the PSTAIRE signals at ~34 kDa were likely to represent CDK2. Similarly, only CDK1 was detected by the PSTAIRE antibodies at ~34 kDa in ^{AID}CDK2^{KO}CDK2 cells. We found that cyclin B-CDK2 was less abundant than cyclin B-CDK1 (Figure 4F, compare ^{AID}CDK1 and CDK2 in cyclin B immunoprecipitates in lane 2). After depletion of CDK1, however, cyclin B-CDK2 accumulated to a level comparable with that of cyclin B-CDK1 in CDK1-containing cells (lane 3).

Finally, we also directly measured the kinase activity of CDK1 and CDK2 using histone H1 as a substrate (Figure 4G). As expected, the kinase activity of CDK1 decreased after silencing of CDK1 in ^{AID}CDK1^{KO}CDK1 cells. Importantly, the kinase activity of CDK2 increased in the absence of CDK1 (during both interphase and mitosis).

Collectively, these data revealed a comprehensive reorganization of cyclin-CDK complexes after the loss of CDK1 or CDK2. In the absence of CDK2, CDK1 assumes the role of a G_1-S CDK by binding to cyclin E. In the absence of CDK1, the increased binding of CDK2 to cyclin B brings cyclin B-CDK2 to a level similar to the original cyclin B-CDK1 to facilitate mitotic entry.

CDK2 generates less mitotic phosphorylation than CDK1

To characterize the relative mitotic phosphorylation induced by CDK1 and CDK2, we released CDK1-containing and -deficient cells from a double-thymidine synchronization before trapping them in mitosis using a microtubule inhibitor. Protein expression was then analyzed after mitotic cells were isolated using

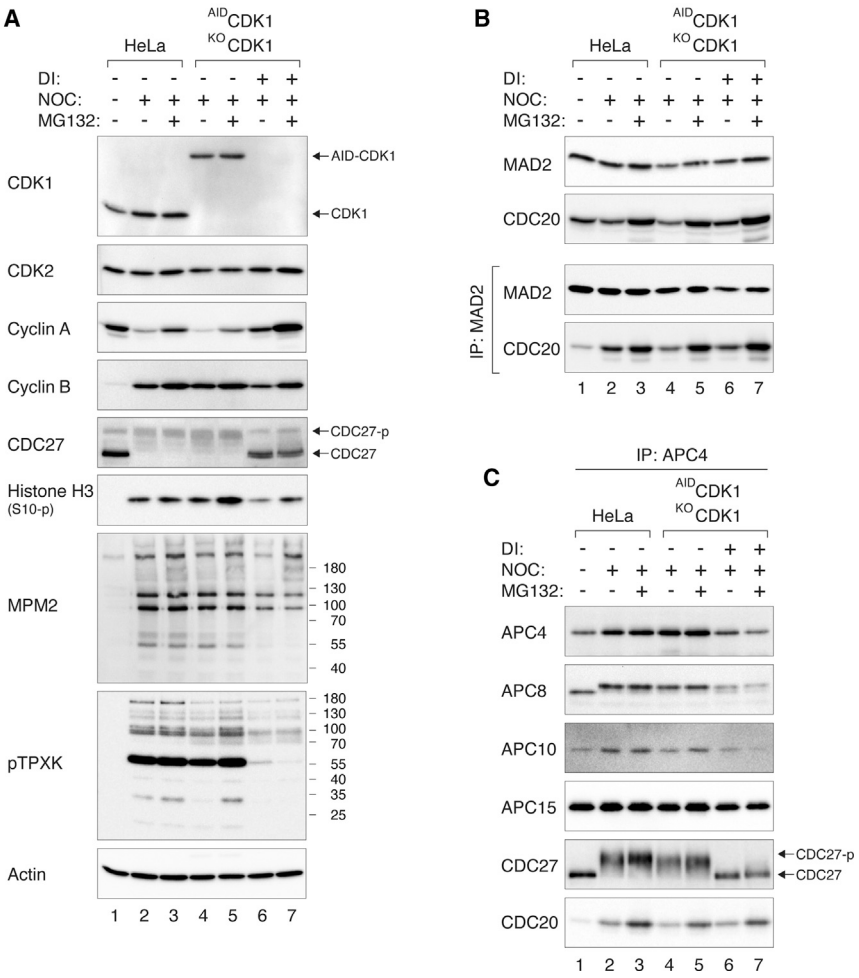

Figure 5. CDK2 generates less mitotic phosphorylation than CDK1

(A) Impaired phosphorylation of specific mitotic substrates in the absence of CDK1. HeLa or ^{AID}CDK1^{KO}CDK1 cells were synchronously released into the cell cycle using a double-thymidine block procedure. DI was added to a portion of the cells to turn off ^{AID}CDK1. After 9 h, NOC was added to trap the cells in mitosis. MG132 was added after 12 h to inhibit the proteasome as indicated. After 15 h, mitotic cells were collected with mechanical shake-off and analyzed with immunoblotting. Lysates from control HeLa cells were loaded in lane 1 to indicate the levels of the proteins in interphase.

(B) CDK1 deficiency does not affect SAC formation. Cells were treated as described in (A). Lysates were prepared and subjected to immunoprecipitation using MAD2 antibodies. The expression of MAD2 and CDC20 was detected with immunoblotting.

(C) Mitotic phosphorylation of APC/C components is diminished in the absence of CDK1. Cells were treated as described in (A). Lysates were prepared and subjected to immunoprecipitation using APC4 antibodies. The expression of different subunits of APC/C and CDC20 was detected with immunoblotting.

mechanical shake-off (Figure 5A). Although CDK1-deficient cells were able to be blocked in mitosis (with high expression of cyclin B and phosphorylated histone H3^{Ser10}), phosphorylation of several CDK substrates were notably lower than in CDK1-catalyzed mitosis. These include CDC27 (an APC/C subunit), MPM2 (a mitotic epitope present in multiple proteins), and a phosphorylated CDK motif (pTPXK). Note that only a subset of proteins recognized by antibodies against MPM2 and pTPXK were reduced in the absence of CDK1. These observations indicated the reduced phosphorylation of many substrates in CDK2-mediated mitosis in comparison with normal mitosis.

Interestingly, the expression of cyclin A (which is normally degraded by APC/C during prolonged mitotic block) was stabilized in the absence of CDK1 (Figure 5A, lanes 4 and 6). The increase in cyclin A was comparable with that when the proteasome was inhibited with MG132 (lanes 5 and 6), suggesting that APC/C-dependent degradation of cyclin A could be less effective in the absence of CDK1. The activity of APC/C is normally inhibited by the spindle-assembly checkpoint (SAC) during mitotic block. To determine whether the SAC was influenced by the absence of CDK1, the binding between MAD2 and CDC20 (part of the mitotic checkpoint complex) was analyzed with co-immunoprecipitation. Figure 5B shows that the amount of MAD2-CDC20 complexes was similar in the presence or absence of CDK1, suggesting the alteration of APC/C activity during CDK2-catalyzed mitosis was not caused by a change in the SAC.

We next investigated whether the APC/C complex could be formed in the absence of CDK1. Figure 5C shows that multiple APC/C subunits (including components of the TPR arm [APC8, APC15, and CDC27], catalytic arm [APC10], and adaptor [CDC20]) could be co-immunoprecipitated with APC4 in the absence of CDK1. Nonetheless, mitotic phosphorylation of several subunits, including APC8 and CDC27, was notably diminished, suggesting that phosphorylation-dependent activation of APC/C could be compromised without CDK1.

Collectively, these results indicate that although CDK2 can drive mitotic entry, inadequate phosphorylation of many substrates could underlie aberrant late mitotic events, such as APC/C activation and cyclin A degradation.

The relatively low abundance of CDK2 accounts for the defective mitotic progression in CDK1-deficient cells

Given that CDK2 was less abundant than CDK1 (Figure 4F), we envisaged that the defective mitosis in CDK1-deficient cells was caused by insufficient CDK2 activities. To test this hypothesis, we overexpressed CDK2-monomeric red fluorescent protein (mRFP) in ^{AID}CDK1^{KO}CDK1 cells (~11× the endogenous CDK2) before ^{AID}CDK1 was turned off (Figure S6A). CDK2-mRFP alleviated the defects observed in CDK1-deficient mitosis

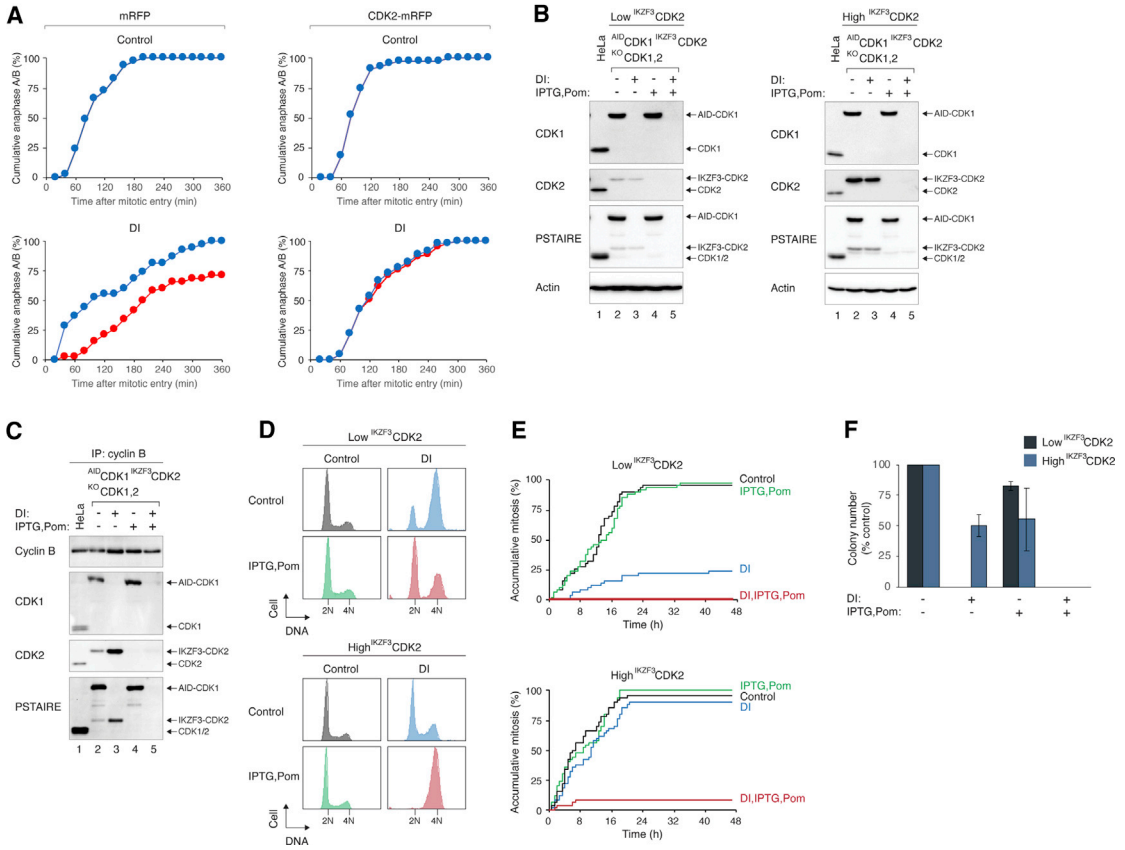

Figure 6. The relatively low abundance of CDK2 accounts for the defective mitotic progression in the absence of CDK1

(A) Ectopic expression of CDK2 reverses anaphase delay in ^{KO}CDK1 cells. ^{AID}CDK1^{KO}CDK1 cells were transfected with either control or CDK2-expressing plasmids. A plasmid expressing histone H2B-GFP was co-transfected as a DNA and co-transfection marker. The cells were incubated with or without DI before being analyzed with live-cell imaging. The time of anaphase A and B relative to mitotic entry time was quantified.

(B) Independent regulation of CDK1 and CDK2 in ^{KO}CDK1,2 cells. ^{KO}CDK1,2 cells expressing ^{AID}CDK1 and ^{IKZF3}CDK2 were generated. ^{IKZF3}CDK2 was expressed either lower or higher than endogenous CDK2. The cells were treated with DI and/or IPTG and Pom for 24 h. Lysates were prepared and analyzed with immunoblotting. Lysates of HeLa cells were loaded to indicate the concentration of endogenous CDK2.

(C) Accumulation of cyclin B-CDK2 upon the loss of CDK1. ^{KO}CDK1,2 cells expressing ^{AID}CDK1 and relatively high expression of ^{IKZF3}CDK2 (B) were treated with DI and/or IPTG and Pom for 24 h. Lysates were prepared and subjected to immunoprecipitation using antibodies against cyclin B followed by immunoblotting.

(D) High expression of CDK2 can compensate for the loss of CDK1. The cells were treated as described in (B) and analyzed with flow cytometry.

(E) Mitotic entry in ^{KO}CDK1 can be restored with ectopically expressed CDK2. ^{KO}CDK1,2 cells expressing ^{IKZF3}CDK2 at concentrations lower or higher than endogenous CDK2 (B) were incubated with DI and/or IPTG and Pom, before being analyzed using live-cell imaging to quantify the percentage of cells entering mitosis. Note that in the absence of CDK1 (DI), mitotic entry occurred normally in cells expressing a relatively high concentration of ^{IKZF3}CDK2.

(F) Expression of CDK2 promotes clonogenic survival in CDK1-deficient cells. ^{KO}CDK1,2 cells expressing ^{AID}CDK1 and different levels of ^{IKZF3}CDK2 were as described in (B). The cells were seeded at low density and grown in the presence of DI and/or IPTG and Pom. After about 2 weeks, the number of colonies was quantified. Interestingly, turning off ^{IKZF3}CDK2 alone also slightly reduced survival, suggesting that these cell lines relied more on CDK2 than control cells. Mean ± SEM of three independent experiments.

(Figure S6B). Figure 6A shows that ectopically expressed CDK2-mRFP largely reversed the delay of anaphase A in CDK1-deficient cells. We also overexpressed a kinase-dead mutant of CDK2 (K33R) in ^{AID}CDK1^{KO}CDK1 cells (Figures S6A and S6B). Mitotic entry was largely abolished after ^{AID}CDK1 was turned off, probably because K33R acted in a dominant-negative manner to prevent endogenous CDK2 from binding to cyclins.

A more rigorous test of the hypothesis would involve expressing CDK2 at different concentrations in an inducible ^{KO}CDK1 background. This prompted us to engineer a system in which CDK1 and CDK2 could be controlled independently. Although CDK1 was controlled by Tet-Off and AID as before, CDK2 was controlled by a LacI-VP64 promoter and an IMiD-responsive IKZF3 degron, allowing CDK2 to be turned off using IPTG and pomalidomide (Pom) (Koduri et al., 2019), respectively (Figure S7A). Figure S7B shows that ^{AID}CDK1 and ^{IKZF3}CDK2 could be destroyed independently using this system.

We further generated cell lines in which ^{IKZF3}CDK2 was expressed at a lower (30%) or higher (~10×) concentration than endogenous CDK2 (Figure 6B). Immunoprecipitation of cyclin B confirmed an increase of cyclin B-^{IKZF3}CDK2 after ^{AID}CDK1 degradation (Figure 6C). The expression of ^{IKZF3}CDK2

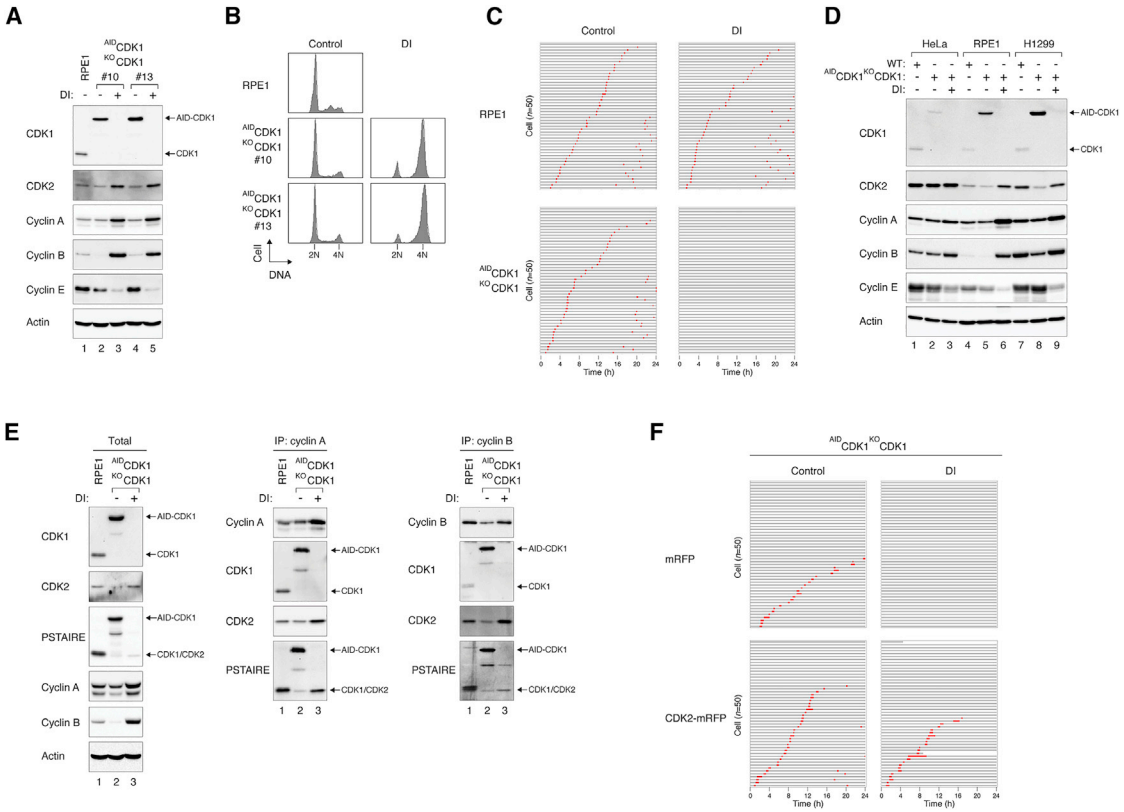

Figure 7. CDK2 is insufficient to drive mitotic entry in RPE1 cells

(A) Conditional silencing of CDK1 in RPE1 cells. WT and ^{AID}CDK1^{KO}CDK1 RPE1 cells (two different clones 10 and 13) were incubated with or without DI. After 24 h, lysates were prepared, and the indicated proteins were detected with immunoblotting. Actin analysis was included to assess protein loading and transfer.

(B) Flow cytometry reveals a 4N DNA cell-cycle arrest after silencing of CDK1 in RPE1. Cells were treated as in (A) and harvested for flow cytometry analysis.

(C) Silencing of CDK1 in RPE1 cells does not induce defective mitosis. WT and ^{AID}CDK1^{KO}CDK1 RPE1 cells were either untreated or incubated with DI before being tracked using live-cell imaging for 24 h. Key: interphase, gray; mitosis, red.

(D) RPE1 contains less cyclin B and CDK2 than cancer cell lines. WT or ^{AID}CDK1^{KO}CDK1 cells from HeLa, RPE1, or H1299 were either untreated or incubated with DI for 24 h. Lysates were prepared and analyzed with immunoblotting.

(E) Binding of CDK2 to mitotic cyclins is insufficient to replace cyclin-CDK1 in RPE1 cells. ^{AID}CDK1^{KO}CDK1 RPE1 cells were incubated with or without DI for 24 h. The expression of the indicated proteins was analyzed with immunoblotting (left panel). Lysates from RPE1 cells were loaded as controls. The lysates were also subjected to immunoprecipitation using antibodies against cyclin A (middle panel) or cyclin B (right panel) before being analyzed with immunoblotting. The PSTAIRE antibody recognized an epitope present in both CDK1 and CDK2.

(F) Overexpressed CDK2 can drive mitosis in CDK1-deficient RPE1. ^{AID}CDK1^{KO}CDK1 RPE1 cells were infected with retroviruses expressing CDK2-mRFP or mRFP. The cells were treated with DI for 24 h before being subjected to live-cell imaging to analyze the fates of mRFP-expressing cells.

determined the position of cell-cycle arrest after both ^{IKZF3}CDK2 and ^{AID}CDK1 were turned off: while cells with relatively low ^{IKZF3}CDK2 expression were arrested mainly in G_1, those with relatively high ^{IKZF3}CDK2 expression were arrested with 4N DNA (Figure 6D). This echoed the above findings that residual CDK1/2 activity was sufficient for G_1-S (Figure 3B).

Turning off ^{AID}CDK1 alone induced a 4N DNA arrest in low ^{IKZF3}CDK2-expressing cells, but not in a background of relatively high ^{IKZF3}CDK2 expression (Figure 6D). Single-cell analysis confirmed that a relatively high concentration of ^{IKZF3}CDK2 enabled entry and exit of mitosis without CDK1, albeit with a longer duration than normal mitosis (Figures 6E and S7C). The ability of overexpressed CDK2 to catalyze a relatively normal mitosis is also consistent with long-term survival (Figure 6F). Clonogenic survival of ^{KO}CDK1 was restored in the presence of overexpressed ^{IKZF3}CDK2 (but not in cells with relatively low expression of ^{IKZF3}CDK2). Not surprisingly, no cells survived after both ^{AID}CDK1 and ^{IKZF3}CDK2 were turned off.

Collectively, these results illustrate that although the normal concentration of CDK2 is insufficient to perform all the mitotic functions of CDK1, overexpressed CDK2 can essentially circumvent the mitotic defects caused by CDK1 deficiency.

Endogenous CDK2 is insufficient to drive mitotic entry in normal RPE1 cells

We next examined whether similar to cancer cell lines, CDK2 can drive mitotic entry in the immortalized normal human epithelial cell line RPE1. ^{AID}CDK1^{KO}CDK1 cells were generated using RPE1 similarly to HeLa or H1299 described above (Figure 7A). Similar to the cancer cell lines, silencing of CDK1 in RPE1 induced a 4N DNA arrest (Figure 7B). This was consistent with the accumulation of G_2-M cyclins (cyclin A and cyclin B) and

reduction of G_1 cyclin E (Figure 7A). To our surprise, single-cell analysis revealed mitotic entry was abolished after ^{AID}CDK1 was destroyed, indicating that RPE1 cells were arrested in G_2 in the absence of CDK1 (Figure 7C). These data suggest that unlike HeLa and H1299, endogenous CDK2 was insufficient to drive mitotic entry in RPE1 cells.

To begin to understand the differences between RPE1 and other cell lines, we next made a side-by-side comparison of the expression of CDKs and cyclins. Intriguingly, although RPE1 expressed only marginally less CDK1 than HeLa or H1299, it expressed notably less CDK2 than the other cell lines (Figure 7D). Likewise, cyclin B was present at a substantially lower concentration in RPE1 in comparison with HeLa or H1299. After turning off ^{AID}CDK1, there was an accumulation of cyclin A-CDK2 and cyclin B-CDK2 complexes in RPE1 ^{AID}CDK1^{KO}CDK1 cells (Figure 7E). Nevertheless, PSTAIRE blotting revealed that the cyclin B-CDK2 complexes were substantially less abundant than cyclin B-CDK1 complexes. This was in marked contrast with HeLa cells, in which the amount of cyclin B-CDK2 complexes after CDK1 depletion was comparable with the original cyclin B-CDK1 (Figure 4F).

Finally, we determined whether ectopically expressed CDK2 could restore mitosis in CDK1-deficient RPE1. Either CDK2-mRFP or mRFP control was expressed in ^{AID}CDK1^{KO}CDK1 RPE1 cells before ^{AID}CDK1 was turned off. The overexpression of CDK2-mRFP is shown in Figure S7D. Tracking the fates of individual mRFP-expressing cells revealed that although mRFP-transfected control cells were prevented from entering mitosis in the absence of CDK1 as anticipated (Figure 7F), CDK2-mRFP-transfected cells were able to enter and exit mitosis normally.

Taken together, these results indicate that unlike cancer cell lines, RPE1 cannot undergo mitotic entry in the absence of CDK1. Probably as a consequence of the relative low concentration of CDK2 in RPE1, the increase in cyclin B-CDK2 complexes after CDK1 destruction was insufficient to initiate mitosis.

DISCUSSION

Progress in the past several years has unraveled some of the underlying principles of the presence of a single type of CDK in yeasts versus multiple CDKs in higher eukaryotes. The fact that all but CDK1 can be deleted in mice without affecting the cell cycle had cast doubt on the unique functions played by some of the CDKs. We confirmed that CDK2 could be deleted without affecting viability in HeLa (Figure 1), H1299 (Figure S1), and RPE1 (unpublished data). In fact, CDK2, CDK4, and CDK6 could be deleted in HeLa without affecting viability (our unpublished data). Also similar to cells from CDK2$^{-/-}$ mice (Aleem et al., 2005), cyclin E was redistributed from CDK2 complexes to CDK1 after CDK2 was destroyed (Figure 4B). Because cyclin A already binds CDK1 under normal circumstances, the increase in cyclin A-CDK1 after CDK2 destruction was less impressive (Figures 4B and 4E). Cyclin A/E-CDK1 presumably was able to replace CDK2 complexes in driving G_1-S and S phase progression. This is in agreement with the observation that ^{KO}CDK2 cells were arrested in G_1-S after CDK1 was also removed (Figure 4).

Although one interpretation of these results is that CDK1 may represent an alternative pathway for regulating G_1-S and S phases, arguments against the hypothesis include the fact that alternative cyclin-CDK complexes, such as cyclin E-CDK1, are formed poorly *in vitro* (Desai et al., 1995) and are not readily detected in cells expressing normal levels of CDK2 (Merrick et al., 2008). In agreement, we also could not detect cyclin E-CDK1 complexes in HeLa unless CDK2 was deleted (Figure 4B). More importantly, experiments in which CDK2 is replaced with an analog-sensitive allele revealed that the activity of CDK2 is essential for both R point and S phase (Merrick et al., 2011), suggesting that CDK1 can replace CDK2's function only when CDK2 protein is reduced to free its cyclin partners.

In contrast with the compensatory roles played by CDK1 in the absence of CDK2, previous evidence suggested that CDK2 cannot replace the functions of CDK1. Knockin mouse in which *Cdk2* was knocked into the *Cdk1* locus resulted in early embryonic lethality (Satyanarayana et al., 2008a). Removal of CDK1 in HT2-19 (one CDK1 allele is disrupted and the other is repressed by a lac repressor) arrested cells in G_2/M (Itzhaki et al., 1997). We verified that downregulation of CDK1 enriched the 4N DNA population (1B, Figures 7B, and S1D). Live-cell imaging, however, revealed different behaviors between normal and cancer cell lines. Although CDK-deficient RPE1 cells were arrested in G_2 (Figure 7C), cancer cells were able to enter mitosis (Figures 2A and 2B). The results in RPE1 resemble that of Cdk1-deficient mouse embryonic fibroblasts (MEFs), which cannot initiate early events of mitotic entry (Diril et al., 2012). Based on evidence including the accumulation of cyclin B-CDK2 complexes (Figures 4 and S5C) and the abrogation of mitosis when CDK2 was also deleted (Figure 3), we believe that at least for cancer cells, the increase in the noncanonical cyclin B-CDK2 was sufficient to trigger mitotic entry. In contrast, RPE1 contained less CDK2 than the cancer cell lines examined here (Figure 7D), which may account for their stalling in G_2 without CDK1 (Figure 7C). Although CDK2 was stabilized after CDK1 depletion in RPE1 (suggesting that forming a complex with cyclin B stabilized CDK2), cyclin B-CDK2 was notably less abundant than cyclin B-CDK1 (Figure 7E).

It is crucial to reiterate that our results were based on rapid depletion of CDK1, which released its cyclin partners to enable them to bind CDK2. Inhibition of the kinase activity of CDK1 with the inhibitor RO3306 (Ma et al., 2009) or the use of an analog-sensitive mutant in chicken DT40 cells (Hochegger et al., 2007) blocked cells in G_2 because cyclin B was presumably unable to redistribute to CDK2. Indeed, inhibition of CDK1 with RO3306 did not increase cyclin B-CDK2 complexes (Figure S5D).

Although CDK2 could initiate mitosis in HeLa and H1299, it was unable to enforce all the mitotic processes normally carried out by CDK1, especially for late mitotic events. Mitosis was extended considerably (Figures 2B and 2D) and was characterized by anaphase B occurring before anaphase A (Figure 2C), oscillation of the metaphase plate (Figure 2E), and precocious cytokinesis (Figures 2D and 2F). The loss of long-term survival (Figure 1D) can be explained by the extensive cell death (Figure 2B) and re-replication (Figure S2C) following the defective mitosis. We reasoned that the difference between CDK2 and

CDK1 in promoting mitosis is quantitative rather than due to a fundamental distinction between the two CDKs. This hypothesis is supported by the observations using PSTAIRE antibodies that CDK2 was expressed at a lower concentration than CDK1 (Figure 4F). This is in agreement with our previous quantitative analysis, indicating that CDK2 is about 10-fold less abundant than CDK1 (Arooz et al., 2000). Significantly, overexpression of CDK2 increased the formation of cyclin B-CDK2 complexes (Figure 6C), re-established normal cell-cycle profile (Figure 6D), and essentially corrected the timing of anaphase A in CDK1-deficient HeLa (Figure 6E). Likewise, overexpression of CDK2 could also drive both entry and completion of mitosis in RPE1 (Figure 7F).

Notwithstanding that the abundance of cyclin B-CDK2 in CDK1-deficient cells was comparable with normal cyclin B-CDK1 (Figure 4F) and active as a kinase *in vitro* (Figure 4G), phosphorylation of specific mitotic substrates was considerably lower in CDK2-mediated mitosis (Figure 5A). These results suggest that the activity of cyclin B-CDK2 may be lower than that of cyclin B-CDK1, which is in agreement with previous *in vitro* analysis of the kinase activity of different cyclin-CDK pairs (Loog and Morgan, 2005; Kõivomägi et al., 2011). It is possible that only with overexpression could CDK2 achieve a sufficient level of substrate phosphorylation to promote late mitotic events.

This line of thought also suggests that early mitotic processes require a lower threshold of CDK activity than late mitotic processes such as anaphase. Although interphase was extended by a couple of hours in the absence of CDK1 (Figure 2A), early mitotic events, including DNA condensation, nuclear envelop breakdown, and metaphase plate formation, were relatively normal once the cell entered mitosis. Activation of APC/C was likely to be impaired, however, as indicated by the severe delay in sister chromatid separation (Figure 2) and stabilization of an APC/C reporter (Figure 2G). Moreover, degradation of cyclin A, which normally occurred during mitotic block, was abolished in the absence of CDK1 (Figure 5A). One mechanism may involve the attenuated phosphorylation of APC/C components, which is a prerequisite for APC/C activity (Yamano, 2019). Indeed, phosphorylation of several subunits, including CDC27 and APC8, was conspicuously downregulated during CDK1-deficient mitosis (Figure 5C).

Another possible reason behind why normal concentration of CDK2 could not completely compensate for the loss of CDK1 may be because of the relatively higher threshold of CDK activity required for mitosis. The idea that a lower threshold of CDK activity is involved in driving S phase compared with that for mitosis was first proposed to explain the presence of the single CDK in yeast (Fisher and Nurse, 1996; Stern and Nurse, 1996; Coudreuse and Nurse, 2010; Swaffer et al., 2016). In metazoan, it is possible that although the activity of CDK2 is adequate for driving S phase, it is insufficient, even when allowed to bind cyclin B, to fulfill all the phosphorylation required for mitosis. In contrast, CDK1 could fully complement the loss of CDK2 both because of the relatively high expression of CDK1 and the low CDK threshold for S phase.

A provocative idea derived from our results is that cancer cells may be more sensitive to downregulation of CDK1 than normal cells. Reducing the expression of CDK1 in cancer cells (e.g., by siRNA) is expected to trigger CDK2-mediated mitosis, which should eliminate most of the cells during the aberrant mitosis or the subsequent interphase. By contrast, normal cells, including RPE1, could be arrested in G_2 without undergoing uncoordinated mitosis, which may enable them to re-enter the cell cycle when the expression of CDK1 is subsequently restored.

STAR★METHODS

Detailed methods are provided in the online version of this paper and include the following:

- KEY RESOURCES TABLE
- RESOURCE AVAILABILITY
  - Lead contact
  - Materials availability
  - Data and code availability
- EXPERIMENTAL MODEL AND SUBJECT DETAILS
- METHOD DETAILS
  - Cell culture
  - Immunofluorescence microscopy
  - Live-cell imaging
  - Flow Cytometry
  - Histone H1 kinase assay
  - Antibodies and immunological methods
- QUANTIFICATION AND STATISTICAL ANALYSIS

SUPPLEMENTAL INFORMATION

Supplemental information can be found online at https://doi.org/10.1016/j.celrep.2021.109808.

ACKNOWLEDGMENTS

This work was supported in part by grants from the Research Grants Council (16100017 to H.T.M.; 16100417, 16103020, and T12-704/16-R to R.Y.C.P.), Health and Medical Research Fund (07183616 to H.T.M.), and Innovation and Technology Commission (ITCPD/17-9 to R.Y.C.P.). We thank Nelson Lee for technical assistance and Toyotaka Ishibashi for helping with the kinase assay.

AUTHOR CONTRIBUTIONS

Conceptualization, H.W.L., H.T.M., T.K.Y., and R.Y.C.P.; methodology, H.W.L., H.T.M., T.K.Y.; investigation, H.W.L., H.T.M., T.K.Y., M.Y.T., D.Z., and S.K.C.; writing, H.W.L., H.T.M., T.K.Y., and R.Y.C.P.; funding acquisition, H.T.M. and R.Y.C.P.; supervision, H.T.M. and R.Y.C.P.

DECLARATION OF INTERESTS

The authors declare no competing interests.

Received: March 1, 2021
Revised: July 19, 2021
Accepted: September 16, 2021
Published: October 12, 2021

REFERENCES

Aleem, E., Kiyokawa, H., and Kaldis, P. (2005). Cdc2-cyclin E complexes regulate the G1/S phase transition. Nat. Cell Biol. *7*, 831–836.

Arooz, T., Yam, C.H., Siu, W.Y., Lau, A., Li, K.K., and Poon, R.Y. (2000). On the concentrations of cyclins and cyclin-dependent kinases in extracts of cultured human cells. Biochemistry *39*, 9494–9501.

Ausubel, F.M., Brent, R., Kingston, R.E., Moore, D.D., Seidman, J.G., Smith, J.A., and Struhl, K. (1995). Current Protocols in Molecular Biology (Wiley Interscience).

Berthet, C., Aleem, E., Coppola, V., Tessarollo, L., and Kaldis, P. (2003). Cdk2 knockout mice are viable. Curr. Biol. *13*, 1775–1785.

Coudreuse, D., and Nurse, P. (2010). Driving the cell cycle with a minimal CDK control network. Nature *468*, 1074–1079.

Desai, D., Wessling, H.C., Fisher, R.P., and Morgan, D.O. (1995). Effects of phosphorylation by CAK on cyclin binding by CDC2 and CDK2. Mol. Cell. Biol. *15*, 345–350.

Dewhurst, M.R., Ow, J.R., Zafer, G., van Hul, N.K.M., Wollmann, H., Bisteau, X., Brough, D., Choi, H., and Kaldis, P. (2020). Loss of hepatocyte cell division leads to liver inflammation and fibrosis. PLoS Genet. *16*, e1009084.

Diril, M.K., Ratnacaram, C.K., Padmakumar, V.C., Du, T., Wasser, M., Coppola, V., Tessarollo, L., and Kaldis, P. (2012). Cyclin-dependent kinase 1 (Cdk1) is essential for cell division and suppression of DNA re-replication but not for liver regeneration. Proc. Natl. Acad. Sci. USA *109*, 3826–3831.

Elledge, S.J., Richman, R., Hall, F.L., Williams, R.T., Lodgson, N., and Harper, J.W. (1992). CDK2 encodes a 33-kDa cyclin A-associated protein kinase and is expressed before CDC2 in the cell cycle. Proc. Natl. Acad. Sci. USA *89*, 2907–2911.

Fisher, D.L., and Nurse, P. (1996). A single fission yeast mitotic cyclin B p34cdc2 kinase promotes both S-phase and mitosis in the absence of G1 cyclins. EMBO J. *15*, 850–860.

Fung, T.K., and Poon, R.Y. (2005). A roller coaster ride with the mitotic cyclins. Semin. Cell Dev. Biol. *16*, 335–342.

Hochegger, H., Dejsuphong, D., Sonoda, E., Saberi, A., Rajendra, E., Kirk, J., Hunt, T., and Takeda, S. (2007). An essential role for Cdk1 in S phase control is revealed via chemical genetics in vertebrate cells. J. Cell Biol. *178*, 257–268.

Itzhaki, J.E., Gilbert, C.S., and Porter, A.C. (1997). Construction by gene targeting in human cells of a "conditional' CDC2 mutant that rereplicates its DNA. Nat. Genet. *15*, 258–265.

Koduri, V., McBrayer, S.K., Liberzon, E., Wang, A.C., Briggs, K.J., Cho, H., and Kaelin, W.G., Jr. (2019). Peptidic degron for IMiD-induced degradation of heterologous proteins. Proc. Natl. Acad. Sci. USA *116*, 2539–2544.

Kõivomägi, M., Valk, E., Venta, R., Iofik, A., Lepiku, M., Morgan, D.O., and Loog, M. (2011). Dynamics of Cdk1 substrate specificity during the cell cycle. Mol. Cell *42*, 610–623.

Lee, M.G., and Nurse, P. (1987). Complementation used to clone a human homologue of the fission yeast cell cycle control gene cdc2. Nature *327*, 31–35.

Li, K.K., Ng, I.O., Fan, S.T., Albrecht, J.H., Yamashita, K., and Poon, R.Y. (2002). Activation of cyclin-dependent kinases CDC2 and CDK2 in hepatocellular carcinoma. Liver *22*, 259–268.

Loog, M., and Morgan, D.O. (2005). Cyclin specificity in the phosphorylation of cyclin-dependent kinase substrates. Nature *434*, 104–108.

Ma, H.T., and Poon, R.Y. (2017). Synchronization of HeLa Cells. Methods Mol. Biol. *1524*, 189–201.

Ma, H.T., Tsang, Y.H., Marxer, M., and Poon, R.Y. (2009). Cyclin A2-cyclin-dependent kinase 2 cooperates with the PLK1-SCFbeta-TrCP1-EMI1-anaphase-promoting complex/cyclosome axis to promote genome reduplication in the absence of mitosis. Mol. Cell. Biol. *29*, 6500–6514.

Mak, J.P.Y., Ma, H.T., and Poon, R.Y.C. (2020). Synergism between ATM and PARP1 Inhibition Involves DNA Damage and Abrogating the G_2 DNA Damage Checkpoint. Mol. Cancer Ther. *19*, 123–134.

Malumbres, M. (2014). Cyclin-dependent kinases. Genome Biol. *15*, 122.

Malumbres, M., Sotillo, R., Santamaría, D., Galán, J., Cerezo, A., Ortega, S., Dubus, P., and Barbacid, M. (2004). Mammalian cells cycle without the D-type cyclin-dependent kinases Cdk4 and Cdk6. Cell *118*, 493–504.

Merrick, K.A., Larochelle, S., Zhang, C., Allen, J.J., Shokat, K.M., and Fisher, R.P. (2008). Distinct activation pathways confer cyclin-binding specificity on Cdk1 and Cdk2 in human cells. Mol. Cell *32*, 662–672.

Merrick, K.A., Wohlbold, L., Zhang, C., Allen, J.J., Horiuchi, D., Huskey, N.E., Goga, A., Shokat, K.M., and Fisher, R.P. (2011). Switching Cdk2 on or off with small molecules to reveal requirements in human cell proliferation. Mol. Cell *42*, 624–636.

Meyerson, M., Enders, G.H., Wu, C.L., Su, L.K., Gorka, C., Nelson, C., Harlow, E., and Tsai, L.H. (1992). A family of human cdc2-related protein kinases. EMBO J. *11*, 2909–2917.

Ng, L.Y., Ma, H.T., Liu, J.C.Y., Huang, X., Lee, N., and Poon, R.Y.C. (2019). Conditional gene inactivation by combining tetracycline-mediated transcriptional repression and auxin-inducible degron-mediated degradation. Cell Cycle *18*, 238–248.

Ninomiya-Tsuji, J., Nomoto, S., Yasuda, H., Reed, S.I., and Matsumoto, K. (1991). Cloning of a human cDNA encoding a CDC2-related kinase by complementation of a budding yeast cdc28 mutation. Proc. Natl. Acad. Sci. USA *88*, 9006–9010.

Ortega, S., Prieto, I., Odajima, J., Martín, A., Dubus, P., Sotillo, R., Barbero, J.L., Malumbres, M., and Barbacid, M. (2003). Cyclin-dependent kinase 2 is essential for meiosis but not for mitotic cell division in mice. Nat. Genet. *35*, 25–31.

Pear, W.S., Nolan, G.P., Scott, M.L., and Baltimore, D. (1993). Production of high-titer helper-free retroviruses by transient transfection. Proc. Natl. Acad. Sci. USA *90*, 8392–8396.

Poon, R.Y. (2016). Cell cycle control: a system of interlinking oscillators. Methods Mol. Biol. *1342*, 3–19.

Poon, R.Y., and Hunter, T. (1995). Dephosphorylation of Cdk2 Thr160 by the cyclin-dependent kinase-interacting phosphatase KAP in the absence of cyclin. Science *270*, 90–93.

Poon, R.Y., Toyoshima, H., and Hunter, T. (1995). Redistribution of the CDK inhibitor p27 between different cyclin.CDK complexes in the mouse fibroblast cell cycle and in cells arrested with lovastatin or ultraviolet irradiation. Mol. Biol. Cell *6*, 1197–1213.

Santamaría, D., Barrière, C., Cerqueira, A., Hunt, S., Tardy, C., Newton, K., Cáceres, J.F., Dubus, P., Malumbres, M., and Barbacid, M. (2007). Cdk1 is sufficient to drive the mammalian cell cycle. Nature *448*, 811–815.

Satyanarayana, A., Berthet, C., Lopez-Molina, J., Coppola, V., Tessarollo, L., and Kaldis, P. (2008a). Genetic substitution of Cdk1 by Cdk2 leads to embryonic lethality and loss of meiotic function of Cdk2. Development *135*, 3389–3400.

Satyanarayana, A., Hilton, M.B., and Kaldis, P. (2008b). p21 Inhibits Cdk1 in the absence of Cdk2 to maintain the G1/S phase DNA damage checkpoint. Mol. Biol. Cell *19*, 65–77.

Stern, B., and Nurse, P. (1996). A quantitative model for the cdc2 control of S phase and mitosis in fission yeast. Trends Genet. *12*, 345–350.

Swaffer, M.P., Jones, A.W., Flynn, H.R., Snijders, A.P., and Nurse, P. (2016). CDK Substrate Phosphorylation and Ordering the Cell Cycle. Cell *167*, 1750–1761.e16.

Woo, R.A., and Poon, R.Y. (2003). Cyclin-dependent kinases and S phase control in mammalian cells. Cell Cycle *2*, 316–324.

Yam, C.H., Siu, W.Y., Lau, A., and Poon, R.Y. (2000). Degradation of cyclin A does not require its phosphorylation by CDC2 and cyclin-dependent kinase 2. J. Biol. Chem. *275*, 3158–3167.

Yamano, H. (2019). APC/C: current understanding and future perspectives. F1000Res. *8*, F1000 Faculty Rev-725.

Yeung, T.K., Lau, H.W., Ma, H.T., and Poon, R.Y.C. (2021). One-step multiplex toolkit for efficient generation of conditional gene silencing human cell lines. Mol. Biol. Cell *32*, 1320–1330.

STAR★METHODS

KEY RESOURCES TABLE

REAGENT or RESOURCE	SOURCE	IDENTIFIER
Antibodies		
beta-actin (mouse monoclonal)	Sigma-Aldrich	Cat# A5316; RRID: AB_476743
APC4 (rabbit polyclonal)	Abcam	Cat# ab72149; RRID: AB_2227064
APC8 (mouse monoclonal)	Santa Cruz Biotechnology	Cat# sc-514006
APC10 (mouse monoclonal)	Santa Cruz Biotechnology	Cat# sc-166790; RRID: AB_2226979
APC15 (mouse monoclonal)	Santa Cruz Biotechnology	Cat# sc-398488
CDC20 (mouse monoclonal)	Santa Cruz Biotechnology	Cat# sc-5296; RRID: AB_628090
BrdU (mouse monoclonal)	DAKO	Cat# M0744; RRID: AB_10013660
CDC27 (mouse monoclonal)	BD Transduction Laboratories	Cat# 610455; RRID: AB_397828
CDK1 (mouse monoclonal)	Santa Cruz Biotechnology	Cat# sc-54; RRID: AB_627224
CDK1 (rabbit polyclonal)	(Li et al., 2002)	N/A
CDK2 (mouse monoclonal)	Santa Cruz Biotechnology	Cat# sc-53220; RRID: AB_629253
CDK2 (rabbit monoclonal)	Abcam	Cat# ab32147; RRID: AB_726775
CDK2 (rabbit polyclonal)	(Li et al., 2002)	N/A
Cyclin A2 (mouse monoclonal)	Tim Hunt (Cancer Research UK)	AT10
Cyclin A2 (rabbit polyclonal)	Proteintech	Cat# 18202-1-AP; RRID: AB_10597084
Cyclin B1 (mouse monoclonal)	Santa Cruz Biotechnology	Cat# sc-245; RRID: AB_627338
Cyclin E1 (mouse monoclonal)	Santa Cruz Biotechnology	Cat# sc-247; RRID: AB_627357
MAD2 (mouse monoclonal)	BD Transduction Laboratories	Cat# 610678; RRID: AB_398005
MPM2 (mouse monoclonal)	Jian Kuang (The University of Texas MD Anderson Cancer Center, USA)	N/A
Pericentrin (rabbit monoclonal)	Abcam	Cat# ab220784
Phospho-CDK substrate [pTPXK] (rabbit monoclonal)	Cell Signaling Technology	Cat# D9V5N; RRID: AB_2798466
Phosphorylated histone $H3^{Ser10}$ (rabbit polyclonal)	Santa Cruz Biotechnology	Cat# sc-8656R; RRID: AB_653256
pRb(Ser807/Ser811-p) (rabbit polyclonal)	Cell Signaling Technology	Cat# 9308; RRID: AB_331472
PSTAIRE (mouse monoclonal)	Masakane Yamashita (Hokkaido University, Japan)	N/A
Chemicals, peptides, and recombinant proteins		
Blasticidin	Thermo Fisher Scientific	CAS: 3513-03-9
Doxycycline	Sigma-Aldrich	CAS: 10592-13-9
G418	Santa Cruz Biotechnology	CAS: 108321-42-2
Hygromycin B	Thermo Fisher Scientific	CAS: 31282-04-9
Indole-3-acetic acid	Sigma-Aldrich	CAS: 87-51-4
Isopropyl β-D-thiogalactopyranoside (IPTG)	Thermo Fisher Scientific	Cat# 15529019
MG132	ApexBio Technology	CAS: 133407-82-6
Nocodazole	Sigma-Aldrich	CAS: 31430-18-9
Pomalidomide	ApexBio Technology	CAS: 19171-19-8
Puromycin	Sigma-Aldrich	CAS: 58-58-2
RO3306	Enzo Life Sciences	CAS: 872573-93-8
Z-VAD-FMK (pan-caspase inhibitor)	Enzo Life Sciences	CAS: 220644-02-0
Critical commercial assays		
Lipofectamine 3000	Thermo Fisher Scientific	Cat# L3000001

(*Continued on next page*)

Continued

REAGENT or RESOURCE	SOURCE	IDENTIFIER
Experimental models: Cell lines		
HeLa (a clone expressing the tTA tetracycline transactivator)	(Yam et al., 2000)	
H1299	American Type Culture Collection	Cat# CRL-5803
RPE1 (a clone immortalized with hTERT)	American Type Culture Collection	Cat# CRL-4000
Oligonucleotides		
See Table S1.		N/A
Recombinant DNA		
See Table S2.		N/A
Software and algorithms		
RStudio (version 1.2.5019)	RStudio	https://www.rstudio.com

RESOURCE AVAILABILITY

Lead contact

Further information and requests for resources and reagents should be directed to and will be fulfilled by the lead contact, Randy Y.C. Poon (rycpoon@ust.hk).

Materials availability

All unique regents generated in this study are available from the lead contact upon request.

Data and code availability

All data reported in this paper will be shared by the lead contact upon request. This paper does not report original code. Any additional information required to reanalyze the data reported in this paper is available from the lead contact upon request.

EXPERIMENTAL MODEL AND SUBJECT DETAILS

HeLa (cervical carcinoma) used in this study was a clone expressing the tTA tetracycline transactivator (Yam et al., 2000). H1299 (non-small cell lung carcinoma) was obtained from American Type Culture Collection (Manassas, VA, USA). RPE1 (retinal pigment epithelial) was a clone immortalized with hTERT (American Type Culture Collection).

^{AID}CDK2^{KO}CDK2 cells from HeLa were generated as previously described (Ng et al., 2019). ^{AID}CDK2^{KO}CDK2 cells from H1299 were generated by transfecting cells with ^{AID}CDK2 in pUHD-SB-AID/Hyg, pSBbi-TIR1-tTA/Pur, CDK2 CRISPR-Cas9, and transposase (pCMV(CAT)T7-SB100) before selection with hygromycin and puromycin for ~2 weeks.

^{AID}CDK1^{KO}CDK1 in HeLa and H1299 were generated as described (Yeung et al., 2021). ^{AID}CDK1^{KO}CDK1,2 cells were generated by transfecting HeLa cells with ^{AID}CDK1 in pUHD-SB-AID/Hyg, CDK1 CRISPR-Cas9, CDK2 CRISPR-Cas9, pSBbi-TIR1/Pur, and transposase (pCMV(CAT)T7-SB100) as appropriate before selection with hygromycin and puromycin for ~2 weeks. ^{AID}CDK1,2^{KO}CDK1,2 cells were generated as described (Yeung et al., 2021).

^{AID}CDK1^{KO}CDK1,2 cells from H1299 were generated by transfecting cells with ^{AID}CDK1 in pUHD-SB-AID/Hyg, pSBbi-TIR1-tTA/Pur, CDK1 CRISPR-Cas9, CDK2 CRISPR-Cas9, and transposase (pCMV(CAT)T7-SB100) before selection with hygromycin and puromycin for ~2 weeks.

^{AID}CDK1^{KO}CDK1 in RPE1 cells were generated by transfecting cells with a mixture of plasmids expressing ^{AID}CDK1 in pUHD-SB-AID/Bla, CDK1 CRISPR-Cas9, TIR1 (pSBbi-TIR1-tTA/Neo), and transposase (pCMV(CAT)T7-SB100) before selection with blasticidin and G418 for ~2 weeks.

^{AID}CDK1^{IKZF3}CDK2^{KO}CDK1,2 cells were generated by transfecting HeLa cells with AID-CDK1 in pUHD-SB-AID/Hyg (Yeung et al., 2021), CDK2-IKZF3 in pIRV-SB-IKZF3/Bla, pSBbi-LacI-VP64-TIR1/Pur, CDK1 CRISPR-Cas9, CDK2 CRISPR-Cas9, and transposase (pCMV(CAT)T7-SB100). The cells were selected with blasticidin, hygromycin B, and puromycin starting from 4 days after transfection. For all the stable cell lines, single cell-derived colonies were obtained by limiting dilution in 96-well plates.

HeLa and RPE1 ^{AID}CDK1^{KO} cell lines expressing CDK2-mRFP, CDK2(K33R)-mRFP, or mRFP were generated by infecting cells with the corresponding retroviruses (viruses were generated in Phoneix-gp cells by co-transfection of CDK2-mRFP in pLNCX2 or mRFP in pLNCX2 with VSV-G (Pear et al., 1993)) in the presence of 5 μg/ml of polybrene (Sigma-Aldrich).

APC/C reporter cells were generated by transfecting ^{AID}CDK1^{KO}CDK1 HeLa cells with plasmids expressing (mRFP)-cyclin B1(CΔ62) and transposase (pCMV(CAT)T7-SB100).

METHOD DETAILS

Cell culture

Cells were propagated in Dulbecco's modified Eagle's medium (DMEM) supplemented with 10% (v/v) calf serum (for HeLa) or fetal bovine serum (for H1299) and 50 U/ml of penicillin streptomycin (Thermo Fisher Scientific, Waltham, MA, USA). RPE1 cells were cultured in DMEM-F12 medium supplemented with 10% (v/v) fetal bovine serum, 50 U/ml of penicillin streptomycin, and 10 μg/ml of hygromycin B. Cells were cultured in humidified incubators at 37°C with 5% CO_2.

Cells were treated with the following reagents at the indicated final concentration: blasticidin (Thermo Fisher Scientific; 3.75 μg/ml), doxycycline (Dox) (Sigma-Aldrich, St. Louis, MO, USA; 2 μg/ml), G418 (Santa Cruz Biotechnology, Santa Cruz, CA, USA; 0.75 mg/ml), hygromycin B (Thermo Fisher Scientific; 0.5 mg/ml), indole-3-acetic acid (IAA) (Sigma-Aldrich; 50 μg/ml), isopropyl β-D-thiogalactopyranoside (IPTG) (Thermo Fisher Scientific; 1 mM), MG132 (ApexBio Technology, Houston, TX, USA; 10 μM), nocodazole (NOC) (Sigma-Aldrich; 100 ng/ml)), pomalidomide (Pom) (ApexBio Technology; 2 μM), puromycin (Sigma-Aldrich; 0.3 μg/ml), RO3306 (Enzo Life Sciences, Farmingdale, NY, USA; 2.5 μM), and Z-VAD-FMK (pan-caspase inhibitor) (Enzo Life Sciences; 10 μM). HeLa and H1299 were transfected using a calcium phosphate precipitation method (Ausubel et al., 1995). RPE1 was transfected using lipofectamine 3000 (Thermo Fisher Scientific).

Synchronization with double thymidine and NOC shake-off were as previously described (Ma and Poon, 2017). For double thymidine synchronization, HeLa cells were grown in medium containing 2 mM of thymidine for 14 h. After washed twice with phosphate-buffered saline (PBS) (170 mM NaCl,3 mM KCl,10 mM Na_2HPO4, and 2 mM KH_2PO4), the cells were incubated in growth medium containing 24 μM of deoxycytidine for 9 h. After further incubation with 2 mM of thymidine for 14 h, the cells were washed twice with PBS, and incubated in growth medium containing 24 μM of deoxycytidine. For NOC shake-off synchronization, cells were first synchronize at early S phase with the double thymidine block procedure. At 2 h after release, the cells were treated with 0.1 μg/ml of NOC and incubated for 10 h. Mitotic cells were collected by mechanical shake-off followed by centrifugation. After washing the cells twice with growth medium by resuspension and centrifugation, the cells were plated in new growth medium.

Cell-free extracts were prepared as described previously (Poon et al., 1995). Briefly, cells were harvested by trypsinization and centrifugation. After washed with PBS and collected by centrifugation, the cells were mixed with twice the pellet volume of a lysis buffer containing 50mM Tris-HCl, pH 7.5, 250 mM NaCl, 5 mM EDTA, 50 mM NaF, 0.2% Nonidet P-40, 1 μg/ml leupeptin, 2 μg/ml aprotinin, 15 μg/ml benzamidine, 10 μg/ml pepstatin, and 10 μg/ml soybean trypsin inhibitor. The suspension was incubated at 4°C for 45 min and cell debris was removed by centrifugation in a microfuge at 4°C for 30 min. The protein concentration of the cell lysate was measured with bicinchoninic acid protein assay system (Pierce, Rockford, IL) using bovine serum albumin (BSA) as a standard.

For colony formation assay, 200-2,000 cells were seeded onto 60-mm plates and treated with the indicated chemicals. After 14 days, colonies were fixed with methanol:acetic acid (2:1 v/v) and stained with 2% (w/v) crystal violet for visualization.

Immunofluorescence microscopy

Cells grown on poly-L-lysine-treated coverslips were fixed with ice-cold methanol at −20°C for 10 min. The cells were then washed three times with phosphate-buffered saline (PBS) for 5 min each time, blocked and permeabilized with 2% bovine serum albumin (BSA) and 0.4% Triton X-100 in PBS at 25°C for 30 min, and washed three times with wash buffer (0.1% Triton X-100 in PBS) for 5 min each time. After incubation with antibodies against pericentrin at 25°C for 60 min, the cells were washed three times with wash buffer, incubated with Alexa Fluor-594 goat anti-rabbit IgG secondary antibodies (Invitrogen) at 25°C for 60 min, and washed another three times with wash buffer. The coverslips were mounted with 2% (w/v) N-propylgallate in glycerol.

Live-cell imaging

Cells were seeded onto 12-well or 24-well cell culture plates and placed into an automated microscopy system with temperature, humidity, and CO_2 control chamber (Zeiss Celldiscoverer 7, Oberkochen, Germany). Images were captured every 5 or 10 min for 24-48 h. Data acquisition was carried out with Zeiss ZEN 2.3 (blue edition) and analysis was performed using ImageJ (National Institutes of Health, Bethesda, MD, USA). After mitosis, one of the daughter cells was randomly selected and continued to be tracked. For cells without histone H2B-GFP, mitosis was defined as from rounding up of cells to the beginning of cytokinesis.

Flow Cytometry

Flow cytometry analysis after propidium iodide staining was performed as previously described (Mak et al., 2020). Briefly, cells were trypsinized and washed with PBS. The cells were then fixed with ice-cold 70% ethanol and stained with a solution containing 40 μg/ml propidium iodide and 40 μg/ml RNaseA at 37°C for 30 min. DNA contents of 10,000 cells were analyzed with FACSAria III (BD Biosciences, Franklin Lakes, NJ, USA).

BrdU incorporation followed by flow cytometry analysis was performed as previously described (Ma and Poon, 2017). Briefly, 10 μM of BrdU was added to cells at 30 min before harvesting. After the cells were harvested, they were incubated with 1ml of freshly diluted 2 M HCl at 25°C for 20 min. After removing the HCl, the cells were incubated with 1 mL of 0.1 M sodium borate at 25°C for 5 min. The cells were then washed once with 1 mL of PBS and once with 1 mL of PBST (PBS with 0.5% Tween 20 and 0.05%w/v BSA). The cells were resuspended in residue buffer and incubated with 2 μl of anti-BrdU antibody (DAKO, Glostrup, Denmark)

at 25°C for 2 h. After washing twice with 1 mL of PBST, the cells were resuspended in residue buffer and incubated with 1 μl of Alexa Fluor-488 goat anti-mouse IgG antibody (Invitrogen) at 25°C for 30 min. After washing twice with 1 mL of PBST, the cells were stained with propidium iodide as above and analyzed with bivariate flow cytometry.

Histone H1 kinase assay

Histone H1 kinase assay was performed as described previously (Poon and Hunter, 1995). Briefly, immunoprecipitates were washed once in H1K buffer (80 mM Na β-glycerophosphate, 20 mM EGTA, 15 mM MgOAc, 1 mM DDT, pH 7.4) and incubated with 10 μl of reaction mix containing 1 μg of histone H1, 50 μM of ATP, and 5% v/v of γ-[^{32}P]-ATP in H1K buffer at 25°C for 10 min. The reaction was terminated by addition of 30 μl of SDS-sample buffer and boiled for 3 min. The samples were applied onto SDS-PAGE. Phosphorylation was detected with a Sapphire Biomolecular Imager (Azure Biosystems, Sierra Trinity, CA, USA).

Antibodies and immunological methods

Immunoblotting was performed as previously described (Ng et al., 2019). Briefly, samples were separated on SDS-PAGE before transferring to Immobilon PVDF membrane (Merck Millipore, Darmstadt, Germany). The membrane was blocked with TBST (10 mM Tris-HCl pH 8.0, 150 mM NaCl, 0.05% Tween-20) containing 4% dry milk or 1% BSA at 25°C for 30 min. The membrane was incubated with primary antibodies in TBST 2% dry milk or 1% BSA at 4°C overnight. After washing with TBST, the membrane was incubated with horseradish peroxidase-conjugated anti-mouse or anti-rabbit immunoglobulin (Thermo Fisher Scientific, Waltham, MA, USA) at 25°C for 2 h. The membrane was then washed three times with TBST, developed using ECL chemiluminescence, and detected using a ChemiDoc Touch imaging system (Bio-Rad, Hercules, CA, USA).

Immunoprecipitation was performed by incubating 400 μg of cell extracts with 1 μl of antiserum or 1 μg of purified antibodies at 4°C for 60 min. The reaction was diluted with 200 μl of bead buffer (25 mM Tris-HCl, pH 7.4, 2.5 mM NaF, 125 mM NaCl, 2.5 mM EDTA, 2.5 mM EGTA, 0.05% Nonidet P-40, 1 μg/ml aprotinin, 7.5 μg/ml benzamidine, 0.5 μg/ml leupeptin, and 5 μg/ml soybean trypsin inhibitor) and added to 10 μl of protein A-Sepharose (GE Heathcare). After incubation at 4°C for 60 min with end-over-end rotation, the beads were spun down in a microfuge and washed four times (1 mL each time) with bead buffer. The beads were then mixed with 35 μl of SDS-sample buffer and boiled for 3 min.

The following antibodies were obtained from the indicated sources: monoclonal antibodies against beta-actin (Sigma-Aldrich), APC8 (sc-514006, Santa Cruz Biotechnology), APC10 (sc-166790, Santa Cruz Biotechnology), APC15 (sc-398488, Santa Cruz Biotechnology), CDC20 (sc-5296, Santa Cruz Biotechnology), CDC27 (610455, BD Transduction Laboratories, Franklin Lakes, New Jersey, USA), CDK1 (sc-54, Santa Cruz Biotechnology), CDK2 (sc-53220, Santa Cruz Biotechnology; or ab32147, Abcam, Cambridge, UK), cyclin A2 (AT10, a gift from Tim Hunt, Cancer Research UK), cyclin B1 (sc-245, Santa Cruz Biotechnology), cyclin E1 (sc-247, Santa Cruz Biotechnology), MAD2 (610678, BD Transduction Laboratories), MPM2 (a gift from Jian Kuang, The University of Texas MD Anderson Cancer Center), pericentrin (ab220784, Abcam), phospho-CDK substrate [pTPXK] (D9V5N from Cell Signaling Technology, Danvers, MA, USA), PSTAIRE (a gift from Masakane Yamashita, Hokkaido University, Japan); polyclonal antibodies against APC4 (ab72149, Abcam), CDK1 (Li et al., 2002), CDK2 (Li et al., 2002), cyclin A2 (18202-1-AP, Proteintech, Rosemont, IL, USA), phosphorylated histone H3^{Ser10} (sc-8656R, Santa Cruz Biotechnology), and pRb(Ser807/Ser811-p) (9308, Cell Signaling Technology).

QUANTIFICATION AND STATISTICAL ANALYSIS

Box-and-whisker plots (center lines show the medians; box limits indicate interquartile range; whiskers extend to the most extreme data points that were no more than 1.5 times the interquartile range from the 25th and 75th percentiles) were generated using RStudio (version 1.2.5019; Boston, MA, USA). Mann-Whitney-Wilcoxon test was used to calculate statistical significance (*$p < 0.05$; **$p < 0.01$). Statistical tests and significance are described in the Figure legends.